Vol. 20, No. 3(2021) Cat1852
Revista Mexicana de Ingeniería Química

Decreasing the value of the cell potential using nPt/C|Ti and RuO_2|Ti as cathodes in a reactor for electro leaching of electronic E-waste

Disminución del valor del potencial de celda utilizando nPt /C|Ti y RuO_2|Ti como cátodos en un reactor para la electrolixiviación de desechos electrónicos

J.C. Ramírez-Castellanos[1], M. Luna-Trujillo[2], V.E. Reyes-Cruz[1], A. Manzo-Robledo[2] , G. Urbano-Reyes[1], M.A. Veloz-Rodríguez[1], J. C. Juárez-Tapia[1], J.A. Cobos-Murcia[1]*

[1] *Universidad Autónoma del Estado de Hidalgo, Área Académica de Ciencias de la Tierra y Materiales, Carr. Pachuca-Tulancingo km 4.5 s/n, Mineral de la Reforma, Hidalgo, México.*
[2] *Instituto Politécnico Nacional. Escuela Superior de Ingeniería Química e Industrias Extractivas, Edificio N 7, Unidad Profesional Adolfo López Mateos. Colonia Lindavista, Del. Gustavo A. Madero, Ciudad de México, CP 07738, México.*

Received: June 27, 2020; Accepted: June 1, 2021

Abstract

In this work, the cell potential during an electrochemical reaction in a separate compartment with anionic-membrane designed for electro-leaching of electronic-waste (E-waste) was studied. For such an approach, in the anode-side the electro-leaching of metals and the oxygen evolution reaction (OER) were monitored using a titanium plate in a HNO3 solution. Whereas, in the cathodic-side three different cathodes (smooth-Pt, titanium coated with ruthenium oxide (RuO_2|Ti) and titanium coated with platinum nanoparticles (nPt/C|Ti)) were used in a solution of H_2SO_4. From the current versus potential characteristics, it has been demonstrated in this work that the modified electrodes promote a better cathodic current for the hydrogen evolution reaction (HER) decreasing the cell potential and then, increasing the current density of the induced metallic electro-leaching in the anode-side. The calculated space-time yield (STY) was ca. 123.4 and 64 $mol.L^{-1}.h^{-1}.cm^{-2}$ for (nPt/C|Ti) and RuO_2|Ti catalysts, respectively. These results put in clear that the use of catalysts at the nano-metric scale could be an interesting alternative to increase the selectivity and conversion of the electro-leaching process at relative low cost.

Keywords: Hydrogen Evolution Reaction, E-waste, electro-leaching, nanoparticles, reactor-design.

Resumen

Este estudio tiene el propósito de disminuir el valor del potencial de celda (E_{cell}) de un reactor electroquímico de compartimentos separados para llevar a cabo la lixiviación de los desechos electrónicos. En el compartimento anódico se utilizó una placa de titanio como ánodo y HNO_3 como anolito. En el lado anódico se evaluó la reacción de evolución de oxígeno (REA) y la electro lixiviación de los metales y en la reacción cátodica la respuesta de tres cátodos diferentes; Platino (Pt), Titanio recubierto con óxido de rutenio (Ti|RuO_2) y Titanio recubierto con nanopartículas de platino(Ti|nPt/C) para la catálisis de la reacción de evolución del hidrógeno (HER) en una solución de H_2SO_4. Los resultados obtenidos por voltamperometría indican que los electrodos modificados con RuO, y nPt/C, promueven una mayor corriente catódica para el HER, disminuyen el potencial de celda y aumentan la densidad de corriente de la electro lixiviación metálica inducida. Esto implica la disminución del potencial eléctrico utilizado por el reactor durante su funcionamiento. Obtención un rendimiento de espacio-tiempo (STY) de 123,4 y 64 $mol.L^{-1}.h^{-1}.cm^{-2}$ para las nanopartículas de carbono y el óxido de rutenio, respectivamente.

Palabras clave: Reacción de evolución de Hidrógenos, E-waste, Electrolixiviación, nPt/C|Ti, Eficiencia Espacio Tiempo.

* *Corresponding author. E-mail*: jose_cobos@uaeh.edu.mx
Tel. +(52)(55) 5804-4720, Fax +(52) (55) 5804-4712
https://doi.org/10.24275/rmiq/Cat1852
ISSN:1665-2738, *issn-e*: 2395-8472

1 Introduction

In recent years, the use of electronic devices has grown exponentially, generating electronic waste called E-waste (López, 2017; López 2016). Metals such as copper, tin, zinc, gold, silver, platinum, rare earth and toxic components as lead, mercury, and cadmium, among others, are contained in these wastes. In this context, some research has focused on the development of metal recovery methods from E-waste (Esparragoza-Montero, 2012; Fogarasi, 2014; Imre-Lucaci, 2017; Kasper, 2016). For example, Au-nanoparticles from this kind of waste could be produced and used as electrodes with good electrochemical responses in drug sensors (Ying, 2020), and in the detection-degradation of organic (or inorganics) compounds from redox reactions (Zhang, 2020, Torres Santillán, 2019). Other studies put in clear that electro-leaching for metal-recovery and pollution control from electrochemical-reactors design is also possible (Torres de la Cruz, 2012; Vargas, 2017).

An important issue of the electrochemical process is the design of reactors; taking into account, for example, the cell potential, (E_{cell}) linked with the applied energy and overpotential (Bard, 2001; Wendt, 1999) during electro-leaching (López, 2017; López 2016).

Also, to decrease this thermodynamic limitations during reactor operation and induces a better selectivity and conversion, energy losses in HER or OER reactions must be considered (De Chialvo, 1999; Pletcher, 2009); in this context, the electrode material plays an important role (i.e. electro-catalysts, Oliver, 2012; Safizadeh, 2015; Tahir, 2017). Thus, to calculate the E_{cell} all electrical contributions presented in the electrochemical system should be considered, Eq. 1 (Pletcher, 1990).

$$E_{cell} = (E_c^{deg} - E_a^{deg}) - |\eta_c| - |\eta_a| - iR_{cell} - iR_{cir} \quad (1)$$

Where E_c^{deg} and E_a^{deg} are the standard cathodic and anodic potential, η_c and η_a the cathode and anodic over-potential, and iR_{cell} and iR_{cir} are the resistances of the cell and the circuit; respectively.

In this way, high electrical resistance can modify the thermodynamic equilibrium in the reactor. At these conditions, it is necessary to overcome these energy barriers to adjust the operating conditions (Bagotsky, 2006; Bockris, 1979). In this context, the HER process occurs through a limited number of steps, represented in Eqs. (2-5). Equation (1) is known as Volmer reaction, where electrochemical adsorption of the proton might occurs. On the other hand, equation (3) is the Heyrovsky mechanism, where desorption is carried out. Whereas, chemical desorption takes place during Tafel reaction, equation (5).

As mentioned above, the first step requires that protons (H^+) adsorb at the electrode surface for direct conversion, Eq. (2). However, other hydrogen-generation phathways are possible according to Eqs. (4) and (5) (Strmcnik, 2016; Eftekhari, 2017; Ortega, 2010).

$$H^+ + e^- \rightarrow H_{ads} \quad (2)$$

$$H^+ + H_{ads} + e^- \rightarrow H_2 \quad (3)$$

$$2H_{ads} \rightarrow H_2 \quad (4)$$

$$H^+_{ads,A} \rightarrow H_2 \quad (5)$$

Metallic substrates (or non-metallic substrates, such as glassy carbon) modified with metallic oxides (or with metallic nanoparticles) are mostly used as electro-catalysts (Lee, 2005; Mateos, 2016). For example, ruthenium oxide (RuO_2) is highly used to produce dimensionally stable anodes (DSA) (Prabhuram, 2003; Terezo, 2002). This kind of catalyst could be an important candidate for using as cathode in metallic electro-leaching reactors.

On the other hand, Pt nanoparticles supported on Vulcan carbon have been alson used as electrocatalysts for proton exchange membrane fuel cells (PEMFC) and electricity generation (Palma, 2018; Alonso, 2006).

In this work materials free of platinum (RuO_2|Ti) were used for the study of the hydrogen evolution reaction (HER). The results were compared with those obtained from smooth-platinum (as a material of reference) and synthesized Pt-nanoparticles supported on Vulcan carbon and deposited on metallic titanium (nPt/C|Ti). On the other hand, the cell potential and kinetic parameters were evaluated during polarization using metallic titanium in the anode-side (separated from the cathode-side throughout an ionic membrane in the electrochemical reactor). It was found that those parameters, during reactor operation, varied with respect to the cathodic material in turn, as has been demonstrated from the E-waste electro-leaching process at bench scale.

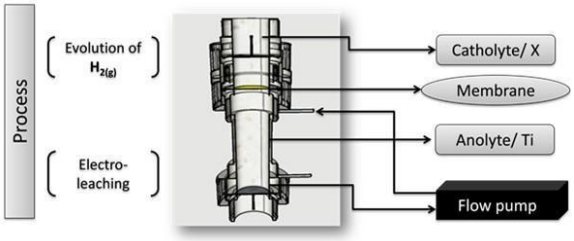

Fig. 1. Scheme of a reactor with separate compartments.

2 Methodology

2.1 *Electrochemical reactor details*

The experimentation was carried out using a cylindrical PVC reactor built in our laboratory, with two compartments separated by an anion exchange polymer membrane (Figure 1). The anolyte-side is localized at the lower segment of the reactor, which presents stationary-diffusion hydrodynamics with an ascending flow (at a rate of 0.725 $cm^3.s^{-1}$) controlled with a peristaltic pump (Master Flex). In this section of the reactor, a disc-shaped titanium plate was used as the anode, which induces the oxidation of electronic waste during an applied potential. In the upper part of the reactor (catholyte-side), which presents non-stationary-diffusion hydrodynamics, three types of electrodes were used as a cathode: a Pt bar, a modified electrodes based on RuO_2|Ti and a synthesized nano-structured material named nPt/C|Ti. The modified RuO_2|Ti electrodes were prepared using a Ti mesh coated with RuO_2 by the Pechini method (Prabhuram, 2003). The modified nPt/C|Ti electrodes were made with platinum nanoparticles supported on Vulcan carbon (nPt/C) and deposited on a titanium mesh according to the literature (Prabhuram, 2003b). Moreover, a saturated Calomel electrode (SCE) immersed in the catholyte-side was used as a reference electrode.

2.2 *Electrochemical reaction procedure*

A HNO_3 solutions were evaluated as an anolyte in concentrations of 2.4 and 0.24 mol $^{-1}$, while the solution in the catholyte was 0.5 $mol.L^{-1}$ H_2SO_4. To evaluate the electrochemical processes, it was necessary to study the cathodic and anodic processes (Figure 2) by placing the working electrode together with the reference electrode in the compartments of interest, obtaining the half-cell potentials for the calculation of the cell potential (According to equation 1).

A potentiostat/galvanostat PAR model 263A was employed. During the cathodic evaluation (Figure 2a), three different arrays were used, referred with the working electrodes in turn. In the first arrangement a Pt bar of 3.32 cm^2 was used as a cathode and a Ti plate of 10.2 cm^2 as anode. This arrangement allows the establishment of a point of comparison in the Ecell with respect to the use of the modified electrodes (RuO_2|Ti and nPt/C|Ti). In the second arrangement, a modified electrode RuO_2|Ti (17.29 cm^2) was used as the cathode and the Ti plate (10.2 cm^2) as the anode; for the third array, a modified nPt/C|Ti electrode was placed as the cathode (17.29 cm ^{2}) and the Ti plate (10.2 cm^2) as the anode. For all cases, an anion-exchange membrane with a polymeric structure of polystyrene gel interwoven with divinylbenzene, a specific functional group of quaternary ammonium, resistivity less than 40 Ω·cm, thermal stability of 90 °C, and ionic permselectivity of 90%, was used (ASTOM, 2019). The linear voltammetry technique was used in a potential window from open circuit potential (OCP) to -600 mV Vs SCE at scan rate of 25 and 50 $mV.s^{-1}$, in order to check charge-transfer process and mass-transport limitation during reaction.

On the other hand, cyclic voltammetry technique was used in potential interval from -250 to 1000 mV at 20 $mV.s^{-1}$ and starting at OCP Vs SCE for 20 cycles to verify the surface state and electrochemical stability of the electrode modified with nPt.

The potential drops of the membrane and the solutions on both the anode side and the cathode side were obtained from the calculation of the IR product, where i is the exchange current and R the resistance of the solution or membrane. For such an approach, the calculated electrolyte resistivity for HNO_3 and H_2SO_4 solutions was 2 and 5 Ω·cm, respectively.

To analyze the process during anodic evaluation (Figure 2b), a Titanium plate was used as the working electrode while the counter electrode was the reference material (Pt) and the synthesized materials (RuO_2 |Ti or nPt/C|Ti). For this case, the reference electrode (SCE) was placed on the anode side. The technique of linear voltammetry was used from the open circuit potential (OCP) to 2500 mV Vs SCE at scan rate of 25 and 50 $mV.s^{-1}$. It is important to mention that by means of the graphic method and using Tafel slopes (not shown), the densities and exchange currents for the study of the cathode and anode processes, were calculated.

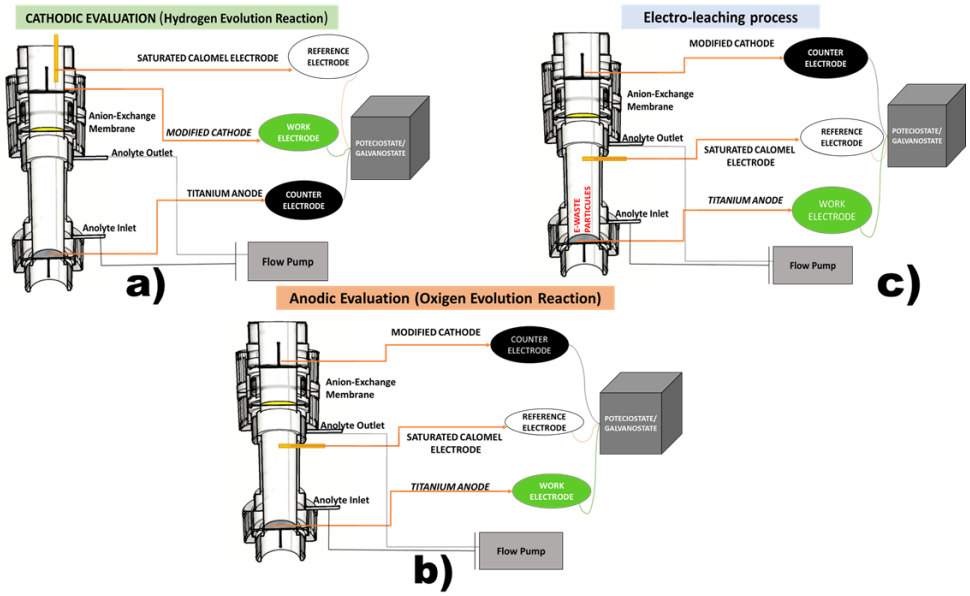

Fig. 2. Scheme of electrochemical process a) Cathodic evaluation, b) Anodic evaluation, and c) Electro-Leaching Process.

Finally, electro-leaching process was evaluated (Figure 2c) using 5 gr of metallic E-waste particles placed on the Ti plate. This sample was used as an anode and the three arrays with three different cathodic electrode-material were analyzed.

The metallic particles were provided by a waste recycling company of electronic equipment and present a heterogeneous morphology (it was not possible to establish the composition in each test) and particle sizes ranging from 1180 to 250 μm as mentioned elsewhere (Ramírez-Castellanos, 2016).

Liquors (leached liquids) obtained from the electro-leaching process were analyzed by Inductively Coupled Plasma Spectroscopy (ICP), Perkin-Elmer model 8300 Optimal 49/5000 model. From each sample, an aliquot of leached liquor in a solution 1/100 was prepared until six solutions of 10 mL corresponding to each experiments were obtained.

The preparation of a calibration curve of 0, 2, 4, 6, 8 and 10 ppm was also carried out using a multi-elemental standard of Au, Ag, Pt, Cu, Ni, Al, Co, Mn, Fe, Pb, Zn and Sn. The computer programs Hydra-Medussa and HSC Chemistry were employed using the Reaction Equations section to analyze the reactions carried out during the electrochemical process in the reactor.

Some reduction and oxidation reactions that occur during electrochemical leaching were established to obtain the corresponding values of electrochemical potential according to the thermodynamics of each reaction.

To determine the space-time performance (g_{sty}), the eq. (7) was used; where gt refers to the amount of moles per liter transformed per unit of time, C_t and C_0 are concentration in a given reaction time and the initial one, respectively. Whereas the concentration (in mole) of formed $H_{2(g)}$ can be calculated using Faraday's law (eq. 6).

$$C_t - C_0 = \frac{i}{zF}dt \tag{6}$$

$$g_{sty} = \frac{i}{zFA}\frac{dt}{t} \tag{7}$$

In equation (6) i (in Amperes) is the current intensity, z (mol) is the number of electrons, F ($C.mol^{-1}$) is the Faraday constant, A (cm^2) is the surface area of electrode, and t (seconds) is the reaction time.

2.3 Morphological characterization of cathodes

2.3.1 X-ray diffraction (XRD)

X-ray diffraction (XRD) technique was used for the phase identification at Pt/C sample. The characteristics of the crystalline structure of the platinum catalyst were determined using a Bruker D-8 diffractometer with a monochromatic Cu K radiation source operated

with a voltage of 35 kV and 25 mA. Phase identification was carried out by comparing the diffractograms of each sample with the JCPDS (Joint Committee for Powder Diffraction Sources) cards. Through the Scherrer equation (eq. 8) the crystallite size was calculated.

$$\beta = \frac{\kappa\lambda}{FWHM(s)\cos(\theta)} \tag{8}$$

Where, β is the particle size, κ is the deformation factor, λ is the wavelengh, θ is the diffraction angle and FWHM (s) is the width of the peak at half the height of the peak.

2.3.2 *Electrochemical Active Surface Area evaluation (ECSA)*

On the other hand, the catalytic and geometric properties determine the activity of some materials. Therefore, one of the most important parameters to define the electrocatalytic activity (i.e., at the surface of Pt particles) is the electrochemical active surface area (ECSA). In this context, the ECSA of the catalysts based on platinum was calculated using the Randles-Sevcik equation (eq. 9).

$$i_p = 2.69 \times 10^5 A D^{1/2} n^{2/3} v^{1/2} C \tag{9}$$

Where i_p= anodic peak current (A), n = Number of electrons transferred, D = Diffusion coefficient ($cm^2 \cdot s^{-1}$), v= scan rate, C = Concentration of $K_3[Fe(CN_6)]$ ($mol \cdot cm^{-3}$) and A = ECSA (cm^2).

For such an approach, a solution of 0.1 $molL^{-1}$ KCl and 5 mM $K_3Fe(CN)_6$ was used for the case of the diffusion coefficient of the mixture KCl and $K_3Fe(CN)_6$. Scans 5, 10, 20, 50, 75, 100 and 120 mVs^{-1} were performed.

3 Results and discussion

3.1 *Structural and morphologial characterization*

3.1.1 *X-ray diffraction (XRD)*

Figure 3 shows the diffraction patterns of the Pt/C electrocatalyst. The diffraction peaks at 2θ= 39.7°, 46.3° and 67.5° degrees, are associated with metallic platinum particles (Gerard, 2002), according with PDF 4-0802, representing a pattern typical of face-centered

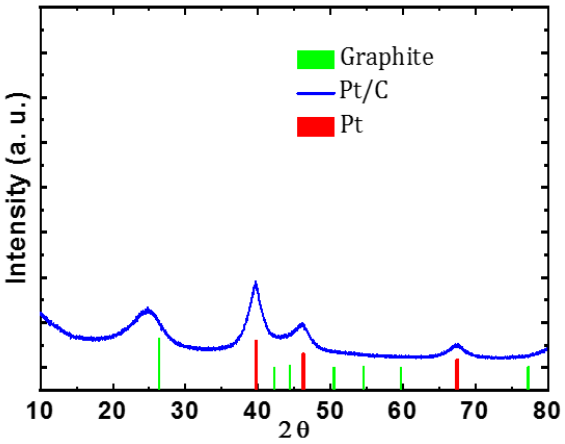

Fig. 3. Diffraction pattern of the Pt/C electrocatalyst.

cubic polycrystalline Pt FCC. The signals for the Pt/C system appearing from 18° to 30° and from 40° to 47° are associated with the short-range ordering of Vulcan carbon coal. According to the Scherrer equation, the crystallite size calculated was 3.5 nm for Pt/C.

From the current versus potential characteristics of Pt, the calculations of the electrochemical active surface area, the number of electrons transferred, reaction kinetics and thickness of the diffuse layer were carry out. The calculated ECSA was 0.257 cm^2.

On the other hand, Ruthenium oxides modified electrode presented a compact-fractured surface, typical of metal oxide coatings obtained by means of thermal decomposition. Also, some particles-agglomerations on the surface were observed. The former were not part of the initial-compact morphology (Gonzales, 2018).

Following with this analysis, smoot-Pt electrode is commonly-used material for electrochemical redox-process, servin as a reference with respect to synthesized material.

3.2 *Electrochemical characterization of the reactor using Pt as cathode*

Figure 4 shows the current-density versus overpotential characteristics (η versus log j) obtained using linear sweep voltammetry during cathodic polarization at a scan rate of 25 and 50 mVs^{-1}. These profiles were obtained using Pt electrode in the catholyte compartment as the working electrode in 0.5 $molL^{-1}$ H_2SO_4 solution. Whereas in the anode-side, a titanium plate served as a counter electrode at two different concentration of HNO_3: (a) 2.4 and (b) 0.24 $molL^{-1}$.

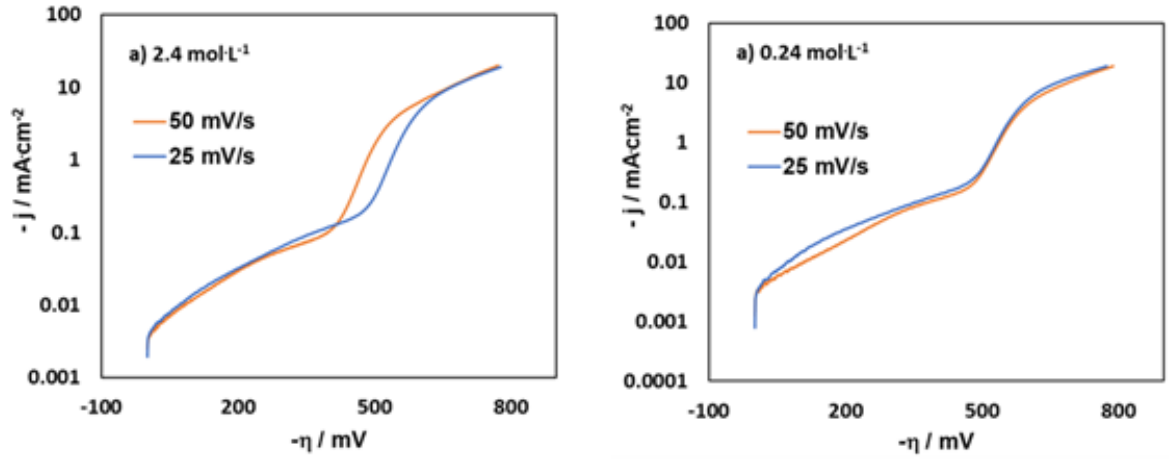

Fig. 4. Current-density versus overpotential characteristics obtained during cathodic polarization using Pt as working electrode in a 0.5 molL^{-1} H_2SO_4 solution. In the anode-side HNO_3 solution at two different concentrations was used as supporting electrolyte.

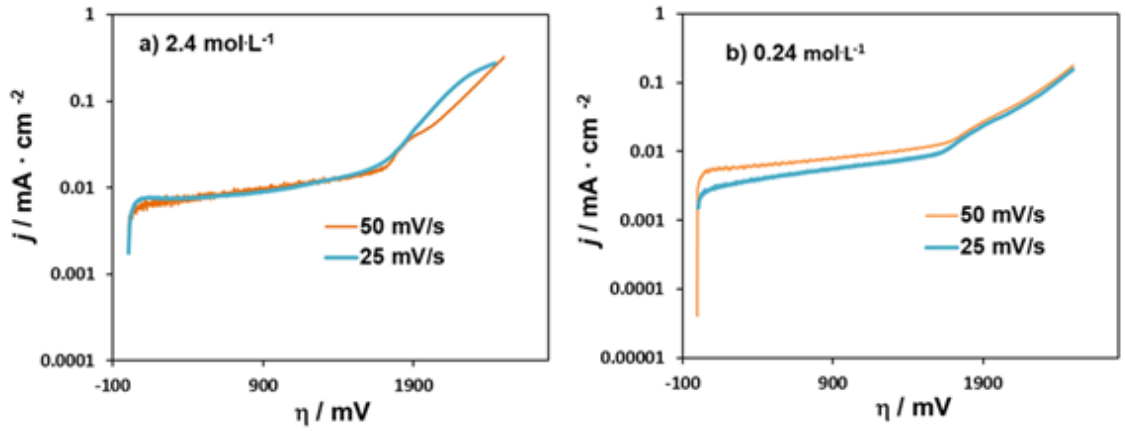

Fig. 5. Current-density versus overpotential characteristics obtained during anodic polarization using Ti as working electrode in a 0.5 molL^{-1} H_2SO_4 solution. In the anode-side HNO_3 solution at two different concentrations was used as supporting electrolyte. See text for details.

The variation in faradaic current, using HNO_3 2.4 mol.L^{-1} as an anolyte (Figure 4a) is attributed to the hydrogen evolution reaction and is observed at both scan rates. The slope changes can be observed at ca. - 420 and - 480 mV during the reduction reaction. The exchange current densities (j_0), calculated were ca. - 0.16 and - 0.31 mA.cm^{-2} for 50 and 25 mVs^{-1}, respectively.

Conversely, for a concentration of 0.24 mol.L^{-1} of HNO_3 (Figure 4b) the reduction process is observed at ca. - 490 mV. For this case, the calculated exchange current density of - 0.31 mAcm^{-2} for both scan rates.

From these results, a slope-variation is observed as a function of anode-side-anolyte concentration and scan rate, improving the HER; moreover, the current density magnitude does not depend on the concentration and/or potential drop caused by solution-resistance in the anode-side. In this context, HER depends only on pH (H_2SO_4 concentration) and electrode nature (catalysts in turn), see below.

On the other hand, the current density versus overpotential characteristics during anodic polarization using a titanium plate as working electrode (instead of platinum, as in Figure 4) are plotted in Figure 5.

For this case, a variation in the faradic current was

observed for both concentrations at potentials from 1.6 V/SCE, associated with oxidation of species at the electrode interface. For example, at 2.4 molL^{-1} of HNO_3 (Figure 5a), nitrate ions (NO_3^-) could be oxidized at both scan rates, generating species such as NO_2 and N_2O_5 at ca. 1.6 and 1.7 mV, respectively. The calculated exchange current (j_0) for both scan rates was ca. -1.7 mAcm^{-2} at 2.4 molL^{-1}; whereas, at 0.24 molL^{-1} the calculated $j_0$was ca. -2 mAcm^{-2}, see Figure 5b.

These results indicate that the current depends on the nitrate-ions concentration, whereas a more positive potentials, the oxygen evolution reaction (OER) takes place. On the other hand, the HER is not affected, within experimental error, with the HNO_3 concentration. However, at low scan rates (i.e., 25 mV s^{-1}) an increment in the faradic current and exchange current was observed. According to this, the concentration of 2.4 molL^{-1} and a scan rate of 25 mVs^{-1} have been selected for experimentation at reactor conditions, see below.

3.3 *Electrochemical characterization of the reactor using modified electrodes as cathode*

Figure 6 shows the current-density versus overpotential characteristics obtained during cathodic polarization using nPt/C|Ti or RuO_2|Ti as working electrode, and Ti as counter electrode. In this array, at the cathode-side a solution of 0.5 molL^{-1} H_2SO_4 was employed, whereas at the anodic-side HNO_3 solutions of 2.4 molL^{-1} (Figure 6a) and 0.24 molL^{-1} (Figure 6b) were used.

From this Figure, both evaluated electrodes show a variation in the slope, linked with a high production of hydrogen on the electrode surface at ca. - 250 mV for RuO_2|Ti and ca. - 160 mV for nPt/C|Ti. For this case, j_0 was ca. - 0.50 and - 0.39 mAcm^{-2}, respectively.

This behavior is mainly associated with the adsorption of protons at the electrode surface (eq. 2), which simultaneously facilitates the process shown in the eq. 3. Thus, it has been demonstrated that titanium electrode modified with platinum nanoparticles (nPt/C) has a better electro-catalytic activity for the hydrogen evolution reaction (HER) compared to the modified RuO_2|Ti electrode and the smooth-platinum electrode. The results corresponding to the exchange current are similar to those reported elsewhere as expected for materials at nano-metric scale.

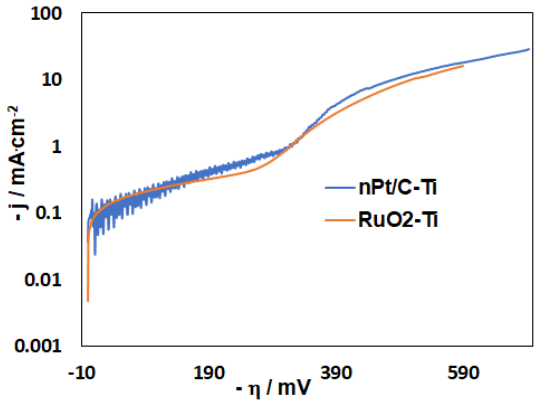

Fig. 6. Current-density versus overpotential characteristics obtained during cathodic polarization using nPt/C|Ti or RuO_2|Ti as working electrode and Ti plate as counter electrode. In the anode side 2.4 molL^{-1} HNO_3 solution; cathode side 0.55 molL^{-1} H_2SO_4 solution. Scan rate of 25 mVs^{-1}.

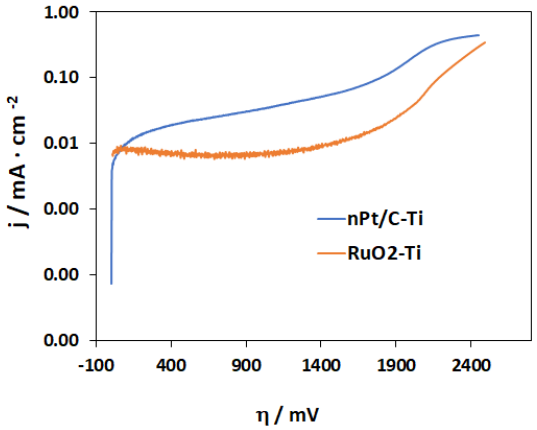

Fig. 7. Current-density versus overpotential characteristics obtained during anodic polarization using nPt/C|Ti or RuO_2|Ti as the working electrode and Ti plate as counter electrode. Solutions: 0.5 molL^{-1} H_2SO_4 in the cathode side; 2.4 molL^{-1} HNO_3 in anode-side. Scan rate of 25 mVs^{-1}.

On the other hand, Figure 7 shows the current-density versus overpotential characteristics obtained during anodic polarization using either RuO_2|Ti or nPt/C|Ti as working electrode and as an anode a Ti plate in a 2.4 molL^{-1} HNO_3 solution as anolyte.

For both electrodes it is possible to observe a variation in the behavior of the anodic slope and in the value of *j*, which could be attributed to the production of oxidized species from the NO_3^- ion, see equations (10-12); with the oxygen evolution reaction at more

anodic potentials (1750 mV for RuO_2|Ti and 1600 mV for nPt/C|Ti), equation (11).

$$2NO^-_{3(aq)} \rightarrow 2NO_{2(g)} + O_{2(g)} + 2e'^- \quad (10)$$

$$4NO^-_{3(aq)} \rightarrow 2N_2O_{5(g)} + O_{2(g)} + 4e^- \quad (11)$$

$$2H_2O_{(l)} \rightarrow O_{2(g)} + 4H^+_{(aq)} + 4e^- \quad (12)$$

The value of j_0 associated with the kinetics of the oxygen evolution reaction (OER) was 0.039 mA.cm^{-2} for Pt/C| Ti and 0.00063 mA.cm^{-2} for RuO_2|Ti, indicating that the charge transfer process is more efficient when compared with that obtained using smooth-Pt as cathode. The cathodic and anodic potential equilibrium and during polarization were obtained from the electrochemical analysis, considering the evolution processes of H_2 and O_2, as shown in Table 1.

The ohmic drop of the catholyte ($IR_{catholyte}$), the anolyte ($IR_{\ anolyte}$) and the membrane ($IR_{membrane}$) were determined from the resistivity of the solutions (nature of the electrolyte-concentration) considering the exchange current in equilibrium conditions and during polarization.

Table 1 shows that the reduction potential using the Pt electrode as cathode was ca. 478 mV Vs SHE; whereas for the oxidation the potential was ca. 277 mV Vs SHE under equilibrium conditions. Also, the calculated potential drop considering an exchange current density of 0.057 mAcm^{-2} was 13.67, - 5.47 and 109.35 mV Vs SHE in the catholyte, anolyte and membrane, respectively.

In addition, the calculated E_{cell} from equation (1) was ca. 637 mV Vs SHE. In the same way, the estimated E_{cell} for the modified electrodes was 481 and 470 mV at equilibrium conditions.

On the other hand, during polarization conditions and with platinum electrode as cathode, the reduction reaction occurs at ca. - 12 mV Vs SHE and the oxidation reaction takes place at 1877 mV Vs SHE.

At the same conditions, the potential drop of the catholyte, anolyte and membrane were ca. 2.37, 0.95 and 18.97 mV Vs SHE, respectively; with a exchange current density of 1 mAcm^{-2}. Also, the calculated E $_{cell}$ was 1845 mV. Whereas the cell potential for the modified electrodes was 1772 and 1729 mV, see Table 1.

According with these results, a decrease in the potential (E_{cell}) between the cathode and the anode is evident, indicating a catalytic effect toward HER for RuO_2|Ti and nPt/C|Ti with respect to smooth-Pt.

From equation (3) and the information obtained using linear voltammetry, the space-time yield (STY) was determined for each counter electrode used; the obtained STY was in the order nPt/C|Ti (123.4) > smooth-Pt (83.1) > RuO_2|Ti (64.0) in molL^{-1}h^{-1}cm^{-2}. Then, the more suitable catalyst is nPt/C|Ti, as expected, whereas RuO_2|Ti presents good activity versus HER.

3.4 Electro-leaching of E-waste on the reactor

Figure 8 shows the response of the E-waste electro-leaching process carried out at titanium anode, in a solution of HNO_3 2.4 molL^{-1} as supporting electrolyte in the anode-side. RuO_2|Ti (Figure 8a) and nPt/C|Ti (Figure 8b) served as cathodes. The response obtained at Ti free of E-waste is shown for comparison.

In a first approach, an increment in current density (j) was observed during electro-leaching of metal particles as a function of the over-potential (η) for both cathodic materials. Interestingly, in absence of E-waste the faradic current is very low, as expected. On the other hand, notice that at nPt/C|Ti electrode, a major current density (ca. 30 mAcm^{-2}) was observed with respect to RuO_2|Ti electrode (ca. 13 mAcm^{-2}).

Table 1. Calculated potential of the compartments and their components under conditions of equilibrium and during polarization.

	Equilibrium Cell (mV vs SHE)			**Polarized Cell (mV vs SHE)**		
	Pt	**RuO_2|Ti**	**nPt/C|Ti**	**Pt**	**RuO_2|Ti**	**nPt/C|Ti**
$E_{\ cathod}$	478	232	175	-12	-19	15
$E_{\ anod}$	277	249	295	1877	1789	1715
$(IR)_{\ cathol}$	13.67	-0.02	-0.0014	2.37	-0.12	-0.1
$(IR)_{\ anol}$	-5.47	0.009	0.0006	-0.95	0.05	0.04
$(IR)_{\ memb}$	109.35	-0.18	-0.0116	18.97	-0.96	0.81
$E_{\ cell}$	637	481	470	1845	1772	1729

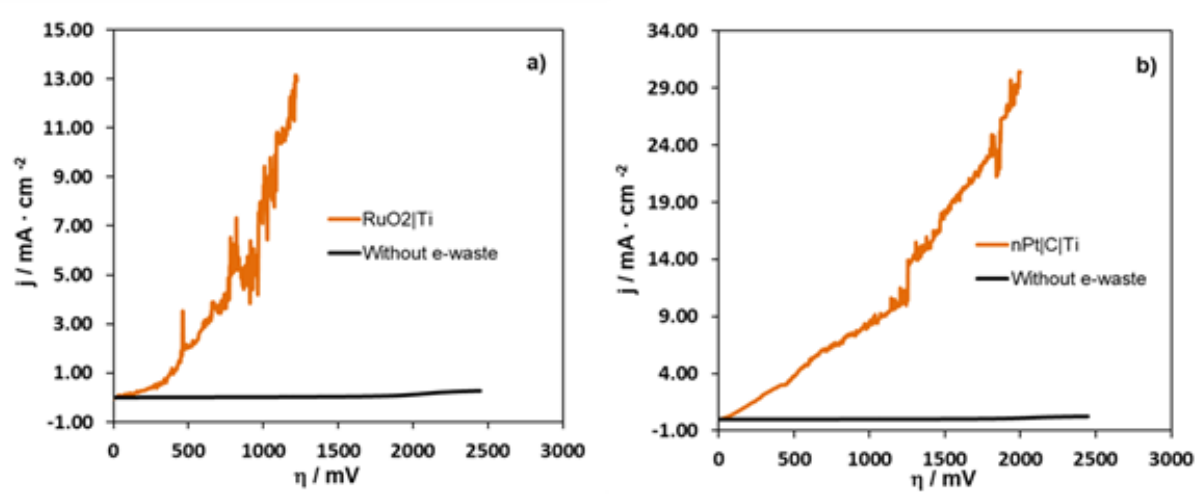

Fig. 8. Anodic response during the electro-leaching process using Ti plate as anode and a) RuO_2|Ti and b) nPt/C|Ti as cathodes in a HNO_3 2.4 molL $^{-1}$ solution. The plots also show the obtained response in absence of E-waste. Scan rate of 10 mVs^{-1}.

Likewise, there were slight changes in slope attributed to the oxidation process of different metals present in E-waste; indicating a better charge transfer in the case of the nPt/C|Ti cathode; and inducing, as a consequence a more efficient anodic reaction, independent of the exchange current.

To determine the amount of electro-leached metals at the supporting electrolyte and during polarization when modified electrodes were used, ICP technique was employed. The results are presented in Table 2.

The data shows that the noble-metals concentration (Ag, Au and Pt) was very similar, although with higher amount of Au when RuO_2|Ti was used.

With the nPt/C|Ti electrode as the cathode, a higher concentration of metals such as Cu, Ni, Fe, Pb, Sn and Zn were obtained. This indicates that the highest anodic current density observed with nPt/C|Ti (Figure 8b) is linked to the oxidation of these metals. Also, it should be noted that the leached amount was in the order Cu > Sn > Zn > Fe for both modified electrodes. Therefore, as observed in Table 2, the selectivity and conversion of the leached products can be modulated from the electrocatalysis-nature in turn.

Then, the HER modulates the leaching process, having major production at modified electrodes, improving the leaching-overpotential in the anodic-side.

Table 2. Concentration (mg.L^{-1}) of metals present in the electro-leaching liquors using the modified electrodes as cathode.

Metals	Concentration [mg.L $^{-1}$]	
	RuO_2|Ti	nPt/C|Ti
Ag	4.1	4.3
Au	5.9	5.6
Pt	0.3	0.4
Cu	707	2106
Ni	162	286
Al	29	40
Co	0	1
Mn	5	21
Fe	572	819
Pb	106	177
Zn	650	649
Sn	1240	1620

Acknowledgements

The authors would like to acknowledge the economic support of the National Council of Science and Technology for the doctoral fellowship and to the Cátedras CONACyT program. JACM Tanks PRODEP 511-6/19-8268. AM-R thanks AIP-SIP-ESIQIE-IPN project 20210066.

Conclusions

The modified electrodes presented a better performance for the hydrogen evolution reaction (HER); and at the same time, the leaching of electronic waste was also improved in the anodic-side. As demonstrated, this better performance is due to the presence of catalytic nanoparticles, affecting the current exchange magnitude, excess potential, and equilibrium potential with respect to smooth-Pt. In this context, the cell potential decreases ca. 73 and 116 mV for RuO_2 |Ti and nPt/C|Ti, respectively. Therefore, the intrinsic catalyst-nature such as morphology, crystalline structure, and particle size linked with the method of synthesis, has an important impact during reaction. The activity of the catalysts based in Pt-nanoparticles was 1.5 times higher with respect to smooth-Pt; whereas the performance for the metal oxide material (with also low cost) was 20% lower; in agreement with the results obtained from STY calculations. On the other hand, during electro-leaching process, high amounts of Cu, Sn, Fe, Ni and Zn with some traces of Pb, Al, Mn, Co, Au, Ag and Pt, were found. Then, the use of modified electrodes based on metallic nanoparticles could be an interesting alternative for pollution control as kinetic parameters and applied energy are enhancing during reaction; and then should be considering for the electrochemical reactors-design to increases selectivity and conversion at low cost.

References

Alonso, V. (2006). Carbonyl tailored electrocatalysts. *Fuel cell 6,* 182-189. https://doi.org/10.1002/fuce.200500245

ASTOM (2019) Corporation Ion exchange membrane (Accessed 17 JANUARY 2019). Available at: http://www.astom-corp.jp/en/product/02.html

Bagotsky, V. (2006). *Fundamentals of Electrochemistry*, 2nd Ed. pp. 34-41. Wiley & Sons, Inc., USA

Bard, A., Faulkner, L., Leddy, J. and Zoski, C. (2001). *Electrochemical Methods: Fundamentals and Applications*, pp. 20-28. John Wiley & Sons, Inc., New York.

Bockris, J.; Reddy, A. (1979). *Modern Electrochemistry: An Introduction to an Interdisciplinary Area*, 1st Ed. Plenum Publishing Corporation, New York, NY, USA; pp. 10-20.

Eftekhari, A. (2017). Electrocatalysts for hydrogen evolution reaction. *International Journal of Hydrogen Energy*, 42, 11053-11077. https://doi.org/10.1016/j.ijhydene.2017.02.125

Esparragoza-Montero, R., Guevara, A., & Torre, E.D. (2012). Recovery of Gold, Silver, Copper and Niobium from Printed Circuit Boards Using Leaching Column Technique. *Journal of Earth Science and Engineering*, 2, 590-595. https://pdfs.semanticscholar.org/dd0f/7fc0080b757cbe5003c231a298e1d69200d3.pdf?_ga=2.41964197.1413784600.1593232981-571061756.1589310462

Fogarasi, S.; Imre-Lucaci, F.; Imre-Lucaci, Á.; Ilea, P. (2014). Copper recovery and gold enrichment from waste printed circuit boards by mediated electrochemical oxidation. *Journal of Hazardous Materials*, 273, 215-221. https://doi.org/10.1016/j.jhazmat.2014.03.043

Fu, L., Zhang, H.Y., Zheng, Y.H., Zhang, H.W. and Liu, Q.H. (2020). An electroanalytical method for brewing vinegar authentic identification. *Revista Mexicana de Ingeniería Química* 19, 803-812. https://doi.org/10.24275/rmiq/Alim869

Gennero de Chialvo, M.R., Chialvo, A. (1999). The Tafel-Heyrovsky route in the kinetic mechanism of the hydrogen evolution reaction. *Electrochemical Communications 1*, 379-382. https://doi.org/10.1016/S1388-2481(99)00078-8

González M. A., Reyes V. E., Cobos J. A., Veloz M. A., Urbano G., Pérez M. (2018). Effect of DSA electrode (A304|RuO2) on the electrochemical production of H_2(g). *International Journal of Electrochemical Science* 13 10873 - 10883, doi: https://doi.org/10.20964/2018.11.58

Gerard, M., Chaubey, A., anda Malhotra, B.D. (2002). Application of conducting polymers to biosensors, *Biosensors and Bioelectronics 17*, 345-359.

Imre-Lucaci, Á.; Nagy, M.; Imre-Lucaci, F.; Fogarasi, S. (2017). Technical and environmental assessment of gold recovery from secondary streams obtained in the processing of waste printed circuit boards. *Chemical Engineering Journal 309*, 655-662. https://doi.org/10.1016/j.cej.2016.10.045

Kasper, A.; Carrillo, A.; Garcia, G.; Veit, M.; Perez, H. (2016). Determination of the potential gold electrowinning from an ammoniacal thiosulfate solution applied to recycling of printed circuit board scraps. *Waste Management & Research*, 34, 47-57. https://doi.org/10.1177/0734242X15607425.

Lee, C.; Ju, Y.; Chou, P.; Huang, Y.; Kuo, L.; Oung, J. (2005). Preparation of Pt nanoparticles on carbon nanotubes and graphite nanofibers via self-regulated reduction of surfactants and their application as electrochemical catalyst. *Electrochemical Communications*, 7, 453-458. https://doi.org/10.1016/j.elecom.2005.01.016

López, C.; Reyes, C.; Veloz, R.; Urbano, R.; Cobos, M.; Nava, M. (2017). Electrochemical Selective Leaching and Deposition of Ag, Au and Pt from electronic waste. *International Journal of Electrochemical Science 12*, 8198-8216. https://doi.org/10.20964/2017.09.45

López, C.; Reyes, V.; Velóz, A.; Hernández, J.; Badillo, F.; Cobos-Murcia, J.A. (2016). Speciation and Characterization of E-Waste, Using Analytical Techniques. In: *Characterization of Minerals, Metals, and Materials*, (Ikhmayies, S), Pp. 629-636. John Wiley & Sons, Switzerland. https://doi.org/10.1007/978-3-319-48210-1_79

Mateos, S.; Hernández, P.; Lartundo, R.; Manzo, R. (2016). Methanol Electro-Oxidation on Pt-Carbon Vulcan Catalyst Modified with WOx Nanostructures: An Approach to the Reaction Sequence Using DEMS. *Industrial & Engineering Chemistry Research 56*, 161-167. https://doi.org/10.1021/acs.iecr.6b02420

Oliver, T.; Arce, E.; Cortés, E.; Bolarín, M.; Sánchez, F.; González, H.; Manzo, R. (2012). Electrochemical behavior of NixW1-x materials as catalyst for hydrogen evolution reaction in alkaline media. *Journal of Alloys and Compounds 536*, 245-249. Elsevier Science, Netherland.

Ortega, C.; Herrera, P.; Verde, G. (2010). Mathematical Modeling of the Hydrogen Evolution Reaction on Pt/C Electrodes Considering Diffusion Effects. *Journal of New Materials for Electrochemical System 13*, 161-229. https://doi.org/10.14447/jnmes.v13i3.171

Palma, G.; Vazquez, A.; Ostos, C.; Manzo, R.; Romero, I.; Calderón, J.; González, I. (2018). In search of the active chlorine species on Ti/ZrO_2-RuO_2-Sb_2O_3 anodes using DEMS and XPS. *Electrochimica Acta* , 275, 265-274. https://doi.org/10.1016/j.electacta.2018.04.114

Pletcher, D. (2009). *A First Course in Electrode Processes*. pp. 5-18,110-125. Royal Society of Chemistry, United Kingdom

Pletcher, D.; Walsh, F. (1990). *Industrial Electrochemistry*, pp. 8-17. Springer, USA

Prabhuram, J.; Wang, X.; Hui, C.; Hsing, I. (2003). Synthesis and characterization of surfactant-stabilized Pt/C nanocatalysts for fuel cell applications. *The Journal of Physical Chemistry B*, 107, 11057-11064. https://doi.org/10.1021/jp0357929

Prabhuram, J.; Wang, X.; Hui, C.; Hsing, I. (2003b). Synthesis and characterization of surfactant-stabilized Pt/C nanocatalysts for fuel cell applications. *The Journal of Physical Chemistry B 107*, 11057-11064. https://doi.org/10.1021/jp0357929

Ramírez, C.; Cobos-Murcia, J.A.; Reyes, V.; Veloz, A.; Urbano, G.; Hernández, J. (2016) (AACTyM-Universidad Autónoma del Estado de Hidalgo). Caracterización de partículas metálicas de E-waste. https://www.uaeh.edu.mx/scige/boletin/aactm/n3/topico1.pdf

Safizadeh, F.; Ghali E.; Houlachi, G. (2015). Electrocatalysis developments for hydrogen evolution reaction in alkaline solutions-a review. *International Journal of Hydrogen Energy 40*, 256-274. https://doi.org/10.1016/j.ijhydene.2014.10.109

Strmcnik, D.; Lopes, P.; Genorio, B.; Stamenkovic, V.; Markovic, N. (2016). Design principles for hydrogen evolution reaction catalyst materials. *Nano Energy*. 29, 29-36. https://doi.org/10.1016/j.nanoen.2016.04.017

Tahir, M.; Pan, L.; Idrees, F.; Zhang, X.; Wang, L.; Zou, J.; Wang, Z. (2017). Electrocatalytic oxygen evolution reaction for energy conversion and storage: A comprehensive review. *Nano Energy 37*, 136-157. https://doi.org/10.1016/j.nanoen.2017.05.022

Terezo, A.; Pereira, E. (2002). Preparation and characterisation of Ti/RuO_2 anodes obtained by sol-gel and conventional routes. *Materials Letters 53*, 339-345. https://doi.org/10.1016/S0167-577X(01)00504-3

Torres de la Cruz, R.; Mejía, J.; Reátegui, R. (2012). Determinación experimental de los parámetros óptimos de operación en el proceso de electrolixiviación y electrodeposición secuencial de oro en soluciones ácidas de Tiourea a partir de sulfuros concentrados. *TECNIA*, 22, 55-64.

Torres-Santillan, E., Vargas-Garcia, J. R., Ramirez-Meneses, E., Manzo-Robledo, A. and Hernandez-Perez, M. A. (2019). Induced electrochemical reduction of nitrates species on interface of Pt/MWCNTs prepared by vapor-phase impregnation-decomposition method. *Revista Mexicana de Ingeniería Química 18*, 431-439. https://doi.org/10.24275/uam/izt/dcbi/revmexingquim/2019v18n2/Torres

Vargas, L.; Rojas, R. (2017). Gold electroleaching in a porous bed reactor. *Revista de la Facultad de Ciencias 6*, 57-6. https://revistas.unal.edu.co/index.php/rfc/article/download/62744/60342

Wendt, H.; Kreysa, G. (1999). *Electrochemical Engineering: Science and Technology in Chemical and Other Industries*. pp. 21-27. Springer-Verlag, Germany. https://doi.org/10.1007/978-3-662-03851-2

Ying, J., Zheng, Y., Zhang, H., and Fu L. (2020). Room temperature biosynthesis of gold nanoparticles with Lycoris aurea leaf extract for the electrochemical determination of aspirin. *Revista Mexicana de Ingeniería Química 19,* 585-592. https://doi.org/10.24275/rmiq/Mat741

Zhang, X., Yang, R. Li, Z., Zhang, M., Wang, Q., Xu, Y., Fu, L., Du, J., Zheng, Y., Zhu, J. and Liu, Q. (2020). Electroanalytical study of infrageneric relationship of Lagerstroemia using glassy carbon electrode recorded voltammograms. *Revista Mexicana de Ingeniería Química 19*, 281-291. https://doi.org/10.24275/rmiq/Bio1750